choose among alternative "compromise" and "limited control" models in which reproductive sharing is determined by the competitive abilities of potential cobreeders. Some of these alternatives yield predictions very different from those offered by the optimal skew model. For example, "restraint" models postulate that subordinates grab the biggest share of the reproductive market possible, restrained only by the threat of expulsion from the group. This pattern is in direct contrast to the optimal skew model, which predicts that subordinates are given a minimum share in reproduction, consistent with the interests of the dominant female (*13*).

Deciding which of these models is correct is already difficult and is likely to become more so as the models increase in complexity to accommodate the findings of new field studies. Already, all possible patterns of reproductive partitioning within groups are compatible with one or more existing skew models (*19*). Even more of a challenge will be to go beyond the qualitative results of Clutton-Brock *et al.* and to quantitatively test alternative skew models. Such tests will be necessary if we are to fully grasp the reasons for the evolution of despotic and egalitarian vertebrate societies.

The meerkat study casts doubt on whether the success of optimal skew theory in explaining differing patterns of reproduction in highly skewed societies such as those of ants can be repeated in the more equitable societies of cooperatively breeding vertebrates. This perhaps should not be surprising. After all, it is in vertebrates that intersexual issues such as mate choice, sexual conflict, biparental care, extra-group matings, and incest avoidance are frequent complications. Given the importance of these factors to social evolution in vertebrate societies, a realistic model of the partitioning of reproductive activities in vertebrates will almost certainly have to take into account interactions between, as well as within, the sexes.

References

1. S. L. Vehrencamp, in *Handbook of Behavior and Communication*, P. Marler, J. G. Vandenbergh, Eds. (Plenum, New York, 1979), vol. 3, pp. 351–394.
2. ———, *Proc. Int. Ornithol. Congr.* **17**, 869 (1980).
3. ———, *Anim. Behav.* **31**, 667 (1983).
4. ———, *Am. Zool.* **23**, 327 (1983).
5. W. D. Hamilton, *J. Theor. Biol.* **7**, 1 (1964).
6. T. H. Clutton-Brock *et al.*, *Science* **291**, 478 (2001).
7. L. Keller, H. K. Reeve, *Trends Ecol. Evol.* **3**, 98 (1994).
8. H. K. Reeve, S. T. Emlen, L. Keller, *Behav. Ecol.* **9**, 267 (1998).
9. H. K. Reeve, P. T. Starks, J. M. Peters, P. Nonacs, *Proc. R. Soc. London Ser. B* **266**, 1 (1999).
10. H. K. Reeve, L. Keller, *Am. Nat.* **150**, S42 (1997).
11. H. K. Reeve, *Am. Nat.* **155**, 365 (2000).
12. M. A. Cant, *Anim. Behav.* **55**, 163 (1998).
13. R. A. Johnstone, M. A. Cant, *Proc. R. Soc. London Ser. B* **266**, 275 (1999).
14. R. A. Johnstone, R. Woodroffe, M. A. Cant, J. Wright, *Am. Nat.* **153**, 315 (1999).
15. H. Kokko, R. A. Johnstone, *Proc. R. Soc. London Ser. B* **266**, 571 (1999).
16. J. E. Ragsdale, *Evol. Ecol. Res.* **1**, 859 (1999).
17. T. H. Clutton-Brock, *Trends Ecol. Evol.* **13**, 288 (1998).
18. T. H. Clutton-Brock *et al.*, *Proc. R. Soc. London Ser. B* **265**, 2291 (1998).
19. R. A. Johnstone, *Ethology* **106**, 5 (2000).

PERSPECTIVES: NANOMATERIALS

Stretching the Mold

Thomas E. Mallouk

Replica molding has long been used to make macroscopic objects—such as bronze statues, plastic dolls, and compact disks—from a mold or master. In this method, the object is formed by injection or chemical synthesis of one material inside the void spaces of another. With the proper choice of materials, this process can faithfully transfer the shape of the mold to the replica even at length scales of a few nanometers. A recent example of chemical replication that pushes the limits of pattern transfer is the successful synthesis of a carbon replica of zeolite Y, a microporous aluminosilicate. The largest pores in the parent material, just 1.3 nm in diameter, are connected by 0.7-nm-wide necks—about the height of two stacked graphite sheets. The carbon is introduced by impregnating the zeolite with furfuryl alcohol, which is first polymerized and then pyrolized. The remaining void space is filled by chemical vapor deposition of carbon from propylene gas. The pure carbon replica, obtained by etching away the aluminosilicate mold with hydrofluoric acid, shows short-range ordering with the same unit cell as the original zeolite (*1*).

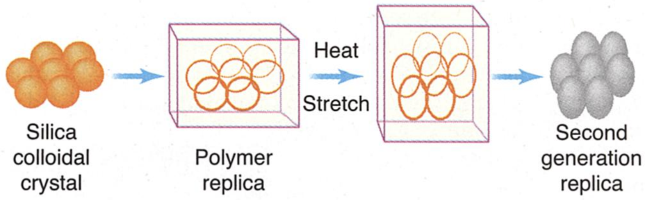

The "lost wax" two-stage replication process. A colloidal crystal of nanoscale silica spheres is converted to a polymer replica, which is then stretched or compressed and filled with a second material. The polymer mold can be removed to give identical free-standing nanoparticles of a wide variety of different materials (*2*).

Recently, replica molding has come into its own as a technique for making nanoparticles in shapes or porous forms that are not accessible by other means. On p. 453 of this issue, Jiang *et al.* describe a two-step process (see the figure) that uses silica (SiO_2) spheres to make a porous plastic replica, which in turn serves as the mold for making solid or hollow particles of a different material—a metal, a metal oxide, a semiconductor, or another polymer (*2*). The plastic mold can be stretched like taffy before it is filled with the second material, resulting in egg-shaped or oblate particles (*3*). Silica is one of the very few materials that allows the facile synthesis of collections of uniform spheres with continuously variable diameters between 30 and 1200 nm. It is thus an ideal master from which to begin the synthesis of spherical and "stretched" nanoparticles of other materials.

The uniform silica spheres used by Jiang *et al.* (*2*) pack into colloidal crystals when a suspension of them is evaporated onto a microscope slide. The spheres are packed tightly just like a stack of cannonballs or a crystal of argon atoms; each sphere has 12 nearest neighbors and together they fill 74% of space. Because the size of the silica spheres is on the order of the wavelength of visible light, these colloidal crystals opalesce; that is, they show diffraction colors in transmitted or reflected light. Colloidal crystals are potentially interesting as photonic band gap materials, which diffract light in much the same way as crystals of atoms diffract electrons (*4*). Given the right crystal structure and a sufficient contrast in refractive index between the nanoparticles and the intervening spaces, light with certain wavelengths cannot propagate in the crystal. Line defects in such crystals should act as low-loss waveguides that can send light around sharp corners, and point defects may be used as laser cavities. The problem is that the two close-packed "cannonball" structures—face-centered cubic and random hexagonal stacking—do not give complete band gaps: Light can leak through the solid along certain crystal directions (*5*). The lowering of symmetry caused by stretching to a lattice of ellipsoids and the increase in contrast afforded by replacing silica with higher index materials could lead to a full photonic band gap in replica colloidal crystals such as those fabricated by Jiang *et al.* (*2*).

There are other compelling reasons for

The author is at the Department of Chemistry, Pennsylvania State University, University Park, PA 16802, USA. E-mail: tom@chem.psu.edu

controlling the precise size and shape of inorganic nanoparticles. One of these can be gleaned from the analogy between colloidal and molecular crystals. Molecules, which always have lower symmetry than spheres, follow the closest packing principle of 12 nearest neighbors but crystallize in lower symmetry (typically monoclinic or triclinic) structures (*6*). The rich variety of molecular crystal structures suggests that something more interesting than cannonball packings may be awaiting colloids of uniform but nonspherical size and shape.

There is also an interesting analogy between the synthesis of asymmetric nanoparticles in polymer molds and the biological synthesis of nanocrystals. The size and shape of the latter are determined by controlled nucleation and growth within bilayer vesicles (*7*). The functional materials (such as sea shells, bones, and teeth) that incorporate these nanocrystals do not have a macroscopic shape that reflects the unit cell of the underlying inorganic material; rather, the nanocrystals are stitched together into hierarchical structures that are programmed by their shape and by their crystal-face–specific interactions with biological macromolecules (*8*).

Much progress has been made in mimicking the process of biomineralization in the laboratory. Furthermore, colloidal nanoparticles can now be made in various symmetric shapes, such as cylinders, prisms, cubes (*9*), and tetrapods (*10*). What we lack, however, is a means of producing nanoparticles with arbitrary asymmetric shapes that might be used to make interlocking structural materials, nanoscale machines, or nanocircuits through self-assembly and colloidal crystallization.

The principles of this kind of assembly are now well established for millimeter-scale objects (hexagons and other shapes), the surfaces of which are derivatized with hydrophilic and hydrophobic materials. When stirred at the interface of two immiscible liquids, these shapes form two-dimensional patterns that minimize the total interfacial free energy (*11*). A similar strategy has been used to direct the growth of three-dimensional crystals from asymmetrically derivatized truncated octahedra (*12*). Noncovalent assembly of this type is likely to scale to nanometer dimensions, as protein assemblies such as flagellar motors and photosynthetic reaction centers demonstrate. It remains to be seen whether the replication of readily available nanoscale objects can be used to fabricate, stretch, and twist molds into the right shape for this kind of synthesis, but the method of Jiang *et al.* is a good start.

References and Notes

1. Z. Ma, T. Kyotani, A. Tomita, *J. Chem. Soc. Chem. Commun.* **2000**, 2365 (2000).
2. P. Jiang, J. F. Bertone, V. L. Colvin, *Science* **291**, 453 (2001).
3. Oblate and prolate polymer ellipsoids have also been obtained by stretching polymer blends (*13*), and similarly shaped inorganic materials have been made by ion bombardment of spherical precursor particles (*14*).
4. E. Jablonovitch, *J. Mod. Opt.* **41**, 173 (1994).
5. K. M. Ho, C. T. Chan, C. M. Soukoulis, *Phys. Rev. Lett.* **65**, 3152 (1990).
6. A. I. Kitaigorodskii, *Chem. Soc. Rev.* **7**, 133 (1978).
7. L. Addadi, S. Weiner, *Angew. Chem. Int. Ed.* **31**, 153 (1992).
8. S. Mann *et al.*, *J. Chem. Soc. Dalton Trans.* **2000**, 3753 (2000).
9. T. S. Ahmadi *et al.*, *Science* **272**, 1924 (1996).
10. L. Manna, E. C. Scher, A. P. Alivisatos, *J. Am. Chem. Soc.* **122**, 12700 (2000).
11. N. B. Bowden, M. Weck, I. Choi, G. M. Whitesides, *Acc. Chem. Res.* 21 December 2000 (http://pubs.acs.org/subscribe/journals/achre4/browse_asap.html).
12. D. H. Gracias *et al.*, *Science* **289**, 1170 (2000).
13. C. C. Ho, A. Keller, L. A. Odell, R. H. Ottewill, *Colloid Polym. Sci.* **271**, 469 (1993).
14. E. Snoeks *et al.*, *Adv. Mater.* **12**, 1511 (2000).

PERSPECTIVES: PLANETARY SCIENCE

The Nightside of Venus

David Crisp

On 20 November 1999, Slanger *et al.* (*1*) pointed the giant, 10-m-diameter, Keck I telescope at the night side of Venus, our closest planetary neighbor. Venus has been scrutinized for 35 years by ground-based telescopes and an armada of spacecraft, but it took just 8 min of exposure time for the high-resolution Keck spectra to yield an important discovery, namely the first evidence for atomic oxygen airglow (*2*) at visible wavelengths on the nightside of Venus. The telltale sign of this airglow was a diffusive emission from the upper atmosphere in the 557.7-nm atomic oxygen green line. This type of emission is prominent in Earth's aurora and diffuse background nighttime airglow, but its appearance in the spectrum of the Venus night sky is surprising for several reasons.

Enhanced online at www.sciencemag.org/cgi/content/full/291/5503/444

Venus was once thought to be Earth's twin because of its similar size and position in the solar system, but closer examination has shown that the two planets differ in just about every aspect, from atmospheric composition to planetary rotation. Unlike Earth's atmosphere, where molecular oxygen (O_2) is a major constituent, the dense, predominately carbon dioxide (CO_2) atmosphere of Venus contains less than ~0.1 part per million of free oxygen, atomic or molecular, above the planet-encircling sulfuric acid clouds (*3*). Atomic oxygen (O) may be produced on the dayside of Venus through photodissociation of CO_2 molecules by ultraviolet sunlight. To produce the observed nightglow, these O atoms must first be transported from the day to the nightside of the planet by the prevailing winds. Once there, they must acquire around 4 eV of excess energy to be excited into the ^1S state. The green line emission is then produced as the excited O atoms each emit a 557.7-nm photon and relax to the ^1D state.

In Earth's atmosphere, O atoms gain the required energy through collisions with energetic electrons from the solar wind or with highly excited O_2 molecules. Neither of these two excitation mechanisms were expected to be very effective on the nightside of Venus because Venus has no de-

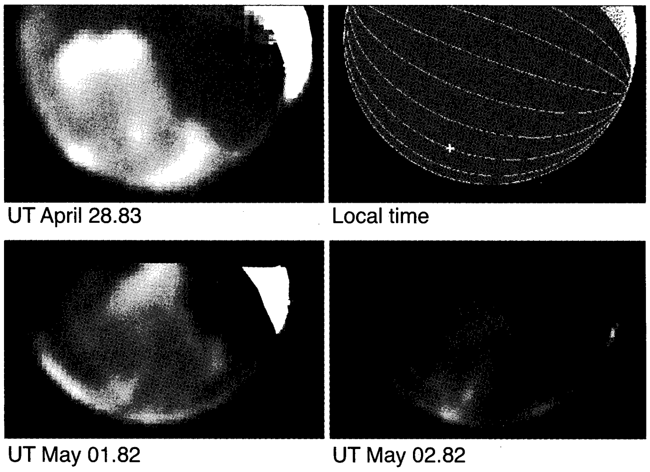
UT April 28.83

Local time

UT May 01.82

UT May 02.82

Mysterious oxygen emission. Spatial and temporal variations in O_2 ($^1\Delta_g$) emission intensity from the nightside of Venus (*8*). The upper right-hand panel shows the orientation of the planet. North is to the lower right, and the illuminated crescent is at the top. The other three images show the airglow distribution on 28 April, 1 May, and 2 May 1993.

The author is with the New Millennium Program, Jet Propulsion Lab, NASA, Pasadena, CA 91109, USA. E-mail: dc@cripsy.jpl.nasa.gov